

E-Cigarette Use, Cigarette Use, and Sex Modify the Nasal Microbiome and Nasal Host-Microbiota Interactions

Elise Hickman

UNC Chapel Hill

Andrew Hinton

UNC Chapel Hill

Bryan Zorn

UNC Chapel Hill

Meghan Rebuli

UNC Chapel Hill <https://orcid.org/0000-0003-1918-2257>

Carole Robinette

UNC Chapel Hill

Matthew Wolfgang

University of North Carolina <https://orcid.org/0000-0003-4534-6470>

Peter Mucha

Dartmouth University

Ilona Jaspers (✉ ilona_jaspers@med.unc.edu)

UNC Chapel Hill

Article

Keywords: E-Cigarettes, nasal microbiome, rRNA

Posted Date: July 20th, 2021

DOI: <https://doi.org/10.21203/rs.3.rs-725763/v1>

License:  This work is licensed under a Creative Commons Attribution 4.0 International License.

[Read Full License](#)

1 **Title:** E-Cigarette Use, Cigarette Use, and Sex Modify the Nasal Microbiome and Nasal Host-
2 Microbiota Interactions

3
4 **Authors:** Elise Hickman^{1,2*}, Andrew Hinton^{3,4,*}, Bryan Zorn⁵, Meghan E. Reboli^{1,2}, Carole
5 Robinette¹, Matthew Wolfgang^{5, 6}, Peter J. Mucha^{3,7}, Ilona Jaspers^{1,2#}

6 *These authors contributed equally to the published work.

7 # Corresponding author

8
9 **Affiliations:**

10 ¹ Center for Environmental Medicine, Asthma, and Lung Biology

11 ² Curriculum in Toxicology & Environmental Medicine

12 ³ Curriculum in Bioinformatics and Computational Biology

13 ⁴ UNC Food Allergy Initiative, School of Medicine

14 ⁵ Marsico Lung Institute

15 ⁶ Department of Microbiology and Immunology

16 ⁷ Department of Mathematics and Department of Applied Physical Sciences

17 University of North Carolina, Chapel Hill, NC, United States

18
19 **Abstract (150-word limit)**

20
21 E-cigarettes are often perceived as safer than cigarettes, but previous research suggests
22 that e-cigarettes can alter respiratory innate immune function. The respiratory microbiome plays
23 a key role in respiratory host defense, but the effect of e-cigarettes on the respiratory microbiome
24 has not been studied. Using 16S rRNA gene sequencing on nasal epithelial lining fluid samples
25 from adult e-cigarette users, smokers, and nonsmokers, followed by novel computational
26 analysis of pairwise log ratios, we determined that e-cigarette use and smoking causes
27 differential respiratory microbiome dysbiosis, which was further affected by sex. We also
28 collected nasal lavage fluid for analysis of immune mediators associated with host-microbiota
29 interactions. Our analysis identified disruption of the relationships between host-microbiota
30 mediators in the nose of e-cigarette users and smokers, which is indicative of disrupted
31 respiratory mucosal immune responses. Our approach provides a novel platform that robustly
32 identifies host immune dysfunction caused by e-cigarette use or smoking.

33
34 **Introduction**

35
36 Approximately 7 million adults and more than 3.5 million youth are current electronic
37 cigarette (e-cigarette) users.¹⁻³ E-cigarettes heat and aerosolize e-liquids containing nicotine and
38 flavorings dissolved in humectants propylene glycol and glycerin. E-cigarette use has been
39 steadily increasing over the past decade, especially among teenagers and young adults, reversing
40 the previous decline in youth tobacco use.^{3,4} Public health crises, such as the outbreak of e-
41 cigarette and vaping-associated lung injury in 2019-2020 and the ongoing SARS-CoV-2 global
42 pandemic, highlight the importance of research examining the effects of e-cigarettes on
43 respiratory immune function.^{5,6}

44 There is emerging evidence that e-cigarettes disrupt respiratory innate immunity.
45 Previous work has demonstrated the potential for e-cigarette toxicity and impairment of
46 respiratory immune defense using *in vitro* and *in vivo* models as well as in samples from human

47 subjects.⁷⁻¹² For example, e-cigarette users have altered markers of innate immune responses in
48 induced sputum and bronchoalveolar lavage fluid in comparison with smokers and
49 nonsmokers,^{8,12} and chronic e-cigarette exposure in mice can dysregulate endogenous lung lipid
50 homeostasis and innate immunity.^{11,13} *In vitro* studies have demonstrated that e-liquids, e-
51 cigarette aerosols, and their components can impair the function of ciliated airway cells and
52 respiratory immune cells.^{9,14-18} Furthermore, e-cigarette exposure has been shown to enhance
53 bacterial virulence and adhesion to airway cells,^{19,20} suggesting that e-cigarette exposure may
54 impact the respiratory microbiome. However, the effects of e-cigarette use on the respiratory
55 microbiome in humans have not been evaluated.

56 The respiratory microbiome includes distinct communities of microbiota along the length
57 of the respiratory tract.²¹ Similar to microbial communities at other body sites, respiratory
58 microbiota interface with the host immune system, and dysbiosis of the respiratory tract
59 microbiome has been associated with diseases, including cystic fibrosis, chronic obstructive
60 pulmonary disease, asthma, and chronic rhinosinusitis, as well as with disease exacerbations and
61 smoking cigarettes.²¹⁻²⁴ Sampling the nasal microbiome is straightforward in contrast to the
62 lower airway microbiome, which is easily contaminated with oral microbiota during specimen
63 collection.²⁵ In addition, the nose is an important gatekeeper in the respiratory tract, as potential
64 pathogens must often colonize this region before progressing to the lower respiratory tract.²¹ This
65 role has become even more clear and relevant with the emergence of SARS-CoV-2, with recent
66 studies showing associations between the nasal microbiome and SARS-CoV-2 infection.^{26,27} Of
67 note is that dysbiosis of the nasal microbiome specifically has been associated with smoking
68 cigarettes,²³ and gene expression and histopathological changes due to smoking are similar in the
69 nasal and lower airway epithelium,⁷ supporting the use of the nasal microbiome for studying the
70 effects of environmental exposures on the respiratory microbiome.

71 Mechanistic study of the human microbiota is an important focus when studying the
72 human microbiome, where identifying microbes associated with disease is paramount.²⁸ To
73 uncover complex interactions in microbiome association studies changes to classical statistical
74 methods are required.²⁹ In addition, computational methods that robustly integrate disparate data
75 types with 16S microbiome data for association testing have been limited.³⁰ In particular,
76 microbiome datasets have interspecies interactions, small sample sizes, high dimensionality
77 (where the number of features greatly exceed the number of samples), are sparse (where the data
78 matrix contains many zeroes), and when converted to relative abundance are compositional,
79 meaning the total number of reads is not informative.³¹ Combined, these challenges significantly
80 confound the multivariate integrative analysis required to improve our understanding of host-
81 microbiome interactions. Thus, novel analytical tools are necessary to uncover true signals
82 hidden within small sample size microbiome data.

83 In this study, we sampled the nasal microbiomes of smokers, nonsmokers, and e-cigarette
84 users using a non-invasive absorptive strip to collect nasal epithelial lining fluid. We then used
85 high-throughput sequencing of the bacterial 16S rRNA gene from the strips to identify bacteria
86 present and analyze the bacterial composition of the nasal microbiome in our subjects. Because
87 these microbial communities are composed of highly interdependent taxa that have complex
88 interaction patterns, multivariate data analysis is critical to extract biologically relevant
89 information.

90 Here, we leverage Selection Energy Permutation³², a novel multivariate association test
91 that simultaneously tests associations while identifying robust subsets of pairwise log ratios in
92 the setting of high-dimensional, low sample size data. These reduced subsets are then used to

93 integratively analyze nasal microbiome and matched cell-free nasal lavage fluid mediator data to
94 determine: 1) whether there were significant compositional differences in the nasal microbiomes
95 of E-cigarette users, smokers, and nonsmokers, 2) whether levels of nasal lavage fluid (NLF)
96 mediators are significantly different in e-cigarette users and smokers in comparison with
97 nonsmokers, and 3) whether changes in levels of these mediators correlate with nasal
98 microbiome dysbiosis. Our data demonstrate nasal microbiome dysbiosis and unique networks of
99 host-microbiota mediators in e-cigarette users and smokers in comparison with nonsmokers. This
100 is indicative of disrupted respiratory mucosal immune responses in these groups and potentially
101 increased susceptibility to infection by specific bacterial taxa. We also observed significant sex
102 differences in the nasal microbiome, highlighting the importance of including sex as a biological
103 variable in nasal microbiome studies.

104

105 Methods

106

107 *Subject recruitment.* Nasal epithelial lining fluid (NELF) strips, nasal lavage fluid (NLF), and
108 venous blood were obtained from healthy adult human e-cigarette users, smokers, and
109 nonsmokers as described previously (**Table 1**),³³ forming our exposure groups. Inclusion criteria
110 were healthy adults age 18-50 years who are either nonsmokers not routinely exposed to
111 environmental tobacco smoke, active regular cigarette smokers, or active e-cigarette users.
112 Active cigarette smoking and e-cigarette use were determined as described previously.⁷
113 Exclusion criteria were current symptoms of allergic rhinitis (deferred until symptoms resolve),
114 asthma, FEV₁ less than 75% predicted at screen, bleeding disorders, recent nasal surgery,
115 immunodeficiency, current pregnancy, chronic obstructive pulmonary disease, cardiac disease,
116 or any chronic cardiorespiratory condition. After the consent process was completed, a medical
117 history and substance use questionnaire was obtained, and subjects were issued a diary to
118 document smoking/vaping for up to 4 weeks, after which they returned for sample collection. E-
119 cigarette users averaged less than 1.5 cigarettes/day in their smoking/vaping diaries, while
120 cigarette users ranged from 4.93-20 cigarettes per day in their diaries. To compare demographic
121 characteristics between subjects in the different exposure groups, age, BMI, and serum cotinine
122 levels were tested for normality using the Shapiro-Wilk test, and groups were compared using
123 the Kruskal-Wallis test followed by the Steel-Dwass method for non-parametric multiple
124 comparisons (analogous to a one-way ANOVA with Tukey's HSD for parametric data).

125

126 *Serum Cotinine Measurement.* Venous blood was collected in BD Vacutainer serum-separating
127 tubes (Fisher Scientific, Waltham, MA) and allowed to clot for a minimum of 15 minutes at
128 room temperature. The blood was then centrifuged at 1200 x g for 10 minutes, and the serum
129 layer was transferred to a fresh tube and stored at -80°C until samples were collected from all
130 subjects. Serum was assayed for cotinine, a metabolite of nicotine that can be measured as a
131 biomarker of nicotine consumption, using a commercially available ELISA kit (Calbiotech,
132 Mannheim, Germany) per manufacturer's instructions. Absorbance was read on a CLARIOstar
133 plate reader (BMG Labtech, Ortenberg, Germany). The limit of quantification for serum cotinine
134 was 5 ng/mL. For samples below the limit of detection, a value of zero was assigned. Serum was
135 not available for one subject in the cohort.

136

137 *NELF Strip Metagenomic Sequencing.* DNA was extracted from whole NELF strips using
138 Powersoil DNA Isolation Kit (MoBio Laboratories). Sequencing libraries were prepared as

139 previously described.³⁴ Samples were sequenced on an Illumina MiSeq kit version V3 2x300
140 paired end over the V3-V4 bacterial 16s gene. Raw sequencing data were demultiplexed and
141 processed to generate a table of operational taxonomic units (OTUs). Specific primer schema,
142 qPCR data, and the OTU table (having at least 10 sequences per OTU across all samples) are
143 provided in the supplement. Raw sequence data have been uploaded under the BioProject
144 accession number PRJNA746950 within the Sequence Read Archive.

145
146 *NLF Processing and Soluble Mediator Measurement.* Cell-free nasal lavage fluid was obtained
147 via processing of raw nasal lavage fluid as described previously.³⁵ Briefly, raw nasal lavage fluid
148 from each nostril was pooled and centrifuged at 500x g through a 40 µm strainer for 10 minutes.
149 Supernatant (cell-free NLF) was collected and stored at -80°C until samples were collected from
150 all subjects. Cell-free NLF was assayed for mediators of host-microbiota interaction (neutrophil
151 elastase, immunoglobulin A (IgA), lactoferrin, lysozyme, interleukin 8 (IL-8), alpha-defensin 1,
152 beta-defensin 1, beta-defensin 2, cathelicidin (LL-37)) using commercially available ELISA kits
153 per manufacturer's instructions as described in Supplementary Table 1. Absorbance was read on
154 a CLARIOstar plate reader. For samples below the limit of detection, a value of ½ the lowest
155 standard was assigned. Cell-free nasal lavage fluid was not available for one subject in the cohort
156 (Figure S1).

157
158 *Sequencing Data Processing and Filtering.* Five samples were removed from the dataset due to a
159 low number of reads (Figure S1). A spiked pseudomonas positive control was identified
160 correctly as pseudomonas. To control for potential contamination on the NELF strips, the
161 decontam R package was used to remove contaminants.³⁶ This package uses an algorithm that
162 takes into account the relative abundance of OTUs in samples and controls to remove the most
163 likely contaminants and has been shown useful for respiratory samples.³⁷ This reduced the
164 number of OTUs from 5346 to 4677. Alpha diversity measures (Observed, Chao1, ACE,
165 Shannon, Simpson, Fisher) were calculated using the phyloseq R library before trimming OTU
166 counts less than 5 for downstream analysis. This brought the number of OTUs to 3059 for
167 downstream analysis.

168
169 *Alpha diversity.* Shannon and Simpson diversity indices were computed for each sample.
170 Diversity indices were tested for normality using the Shapiro-Wilk test and further statistical
171 tests to compare groups were carried out using the appropriate parametric (two-tailed t-test,
172 ANOVA) or non-parametric (Kruskal-Wallis, Steel Dwass) tests. These analyses were performed
173 using JMP Pro 14 and GraphPad Prism 8.

174
175 *Nasal Microbiome Compositional Data Analysis.* To limit spurious findings and because
176 absolute sequencing counts are uninformative,^{31,38,39} compositional data analysis (CoDA)⁴⁰ was
177 carried out on the OTU count table after aggregating OTUs ($O = 3059$) by family (min. level
178 assigned) and genera (max level assigned) and removing taxa not present in at least 20% of
179 samples. The 20% sparsity threshold was selected to maximize class-specific information (Sex,
180 Exposure group) while ensuring the microbial signatures were robust and contained minimal
181 noise due to excessive sparsity. After aggregating OTUs, we define the taxa count matrix, $\mathbf{X} \in$
182 $\mathbb{R}^{n \times p}$, with $n = 62$ samples and $p = 143$ taxa. The closure operator, $C[\cdot]$, was then used to map
183 the count data of each element x_{ij} of \mathbf{X} onto its corresponding coordinate on the unit-sum
184 simplex, defining $\mathbf{X}' = C[\mathbf{X}]$ in terms of matrix elements as

185

$$186 \quad x'_{ij} = (C[\mathbf{X}])_{ij} = \frac{x_{ij}}{\sum_{k=1}^p x_{ik}}$$

187

188 Because the presence of zeros is a major limitation of the log ratio transformation essential to
 189 CoDA, all zeroes must be robustly imputed to non-zero values. To overcome this we use the
 190 ratio-preserving multiplicative replacement strategy which has been shown to have several
 191 theoretical advantages over simple additive replacement:⁴¹ we set the δ imputed values to a
 192 single constant equal to the smallest nonzero value encountered in \mathbf{X}' . From this, we impute
 193 zeros and replace \mathbf{X}' with \mathbf{Z} defined in matrix elements as:

194

$$195 \quad z_{ij} = \begin{cases} \delta & , \quad x'_{ij} = 0 \\ \left(1 - \sum_{k|x_{ik}=0} \delta\right) x'_{ij} & , \quad x'_{ij} > 0 \end{cases}$$

196

197 *Partial redundancy analysis to remove variation due to Sex.* To remove the significant effect of
 198 Sex (which otherwise obscures the exposure group effect) on \mathbf{Z} , partial Redundancy Analysis
 199 (pRDA)⁴² was used. Here we encode the Sex variable into the design matrix \mathbf{S} . Additionally, to
 200 ensure multiple regression computations used in pRDA are performed on symmetric vectors in
 201 real space that preserves the inter-sample Euclidean distances, a center log ratio (clr)
 202 transformation was applied⁴⁰ to \mathbf{Z} , defining the clr values \mathbf{C} for each sample as $\mathbf{c}_i = [c_1, \dots, c_p]$
 203 such that:

204

$$205 \quad c_{ij} = \log\left(\frac{z_j^i}{G_i}\right) \text{ where } G_i = \left(\prod_j z_{ij}\right)^{\frac{1}{p}}$$

206

207 With \mathbf{C} defined, pRDA was carried out in the vegan R package.⁴³ Multivariate linear regression
 208 of \mathbf{C} on \mathbf{S} (i.e. computed as a series of multiple linear regression on individual features) was used
 209 to produce the fitted values $\widehat{\mathbf{C}}$. To remove the Sex effect as in pRDA, the adjusted values of \mathbf{C}
 210 were computed by $\mathbf{P} = \mathbf{C} - \widehat{\mathbf{C}}$ where $\widehat{\mathbf{C}}$ contains all variation attributable to Sex. With \mathbf{P} defined
 211 in Euclidean coordinates which are not suitable for downstream pairwise log ratio
 212 transformations, an inverse clr transformation was applied to map the adjusted coordinates back
 213 to the unit-sum simplex. The Sex adjusted relative abundance matrix \mathbf{M} with elements m_{ij} is
 214 computed as:

215

$$216 \quad m_{ij} = \frac{\exp(p_{ij})}{\sum_{k=1}^p \exp(p_{ik})}$$

217

218 *Nasal Microbial Signature identification using Selection Energy Permuation.* To identify
 219 microbial log ratio signatures in the setting of high-dimensional low sample size data we utilized
 220 the recently developed Selection Energy Permutation (SelEnergyPerm) method, which has been
 221 shown to have increased statistical power over several existing multivariate hypothesis testing

methods under hypothesis testing settings like this.³² The SelEnergyPerm method simultaneously selects a reduced subset of log ratios while maximizing the association between groups. Let the group distributions be defined as $X \in \mathbb{R}^{n \times f}$ and $Y \in \mathbb{R}^{m \times f}$. In this work, we use SelEnergyPerm with the energy statistic (E-statistic)⁴⁴ defined by

$$\mathcal{E}_{n,m}(X, Y) = 2A - B - C,$$

where A, B, and C are specified, in terms of the vectors of \mathbb{R}^f indexed by sample, by

$$A = \frac{1}{nm} \sum_{i=1}^n \sum_{j=1}^m \|x_i - y_j\|, \quad B = \frac{1}{n^2} \sum_{i=1}^n \sum_{j=1}^n \|x_i - x_j\|, \quad C = \frac{1}{m^2} \sum_{i=1}^m \sum_{j=1}^m \|y_i - y_j\|$$

From this, the pooled multi-class (#classes ($c \geq 2$) E-statistic becomes

$$S = \sum_{1 \leq j < k \leq k} \left(\frac{n_j + n_k}{2N} \right) \left[\frac{n_j n_k}{n_j + n_k} \mathcal{E}_{n_j, n_k}(X_j, X_k) \right]$$

The pooled E-statistic is then maximized using forward selection on a subset selected from the full set of pairwise log ratios to explain maximal variation when compared to the full set of pairwise log ratios. Similar to the approach in Greenacre et al.,⁴⁵ the reduced subset of log ratios are selected from the $\frac{p(p-1)}{2}$ 2-dimensional feature space (all pairs). However, there are p^{p-2} possible ways to select a subset of log ratios that explain the total log ratio variance. To overcome this, SelEnergyPerm scores each log ratio using the differential compositional variation scoring method and then iteratively computes acyclic subsets of log ratios,³² with permutation testing via Monte Carlo sampling⁴⁶ to assess the significance and prevent overfitting of the log ratio signature. Specifically, given a log ratio signature discovered with true labels, SelEnergyPerm tests if the observed pooled E-statistic (S^*) is more extreme than E-statistics sampled from the permutation distribution of log ratio signatures selected under random labels (S_i , indexing different random-label samples). With γ such E-statistics randomly sampled from the permutation distribution the one-sided p-value becomes

$$\hat{p} = \frac{1 + \sum_{i=1}^{\gamma} I(S_i > S^*)}{\gamma + 1}$$

As expected, we find that removing large numbers of uninformative features increases statistical power in the high-dimensional low-sample-size setting. To identify the Sex nasal microbial signatures in this study we utilized **Z** with labels = *Sex* and for the Exposure group microbial signature we utilized **M** with labels = *Subject Group*. Using these data, we applied the SelEnergyPerm method with default settings using 200 permutations. Additionally, to reduce noise from sparse features, we further reduced taxa included in the analysis by first identifying the number of taxa to include in the microbial signature. We tested the following subset sizes: [5,10,20,40,60,80,100]. Applying the SelEnergyPerm method on each subset and normalizing the energy statistic⁴⁴ we selected the subset that maximized the normalized pooled energy statistic (**Figure S2**) and then tested if the observed S^* was more extreme than random. In

258 this way, we increase the statistical power of our analysis and reduce the chance of overfitting.
259 While this is good for identifying associations, it can come at the expense of reduced overall
260 discriminatory potential.

261
262 *Network Visualization of Microbial signature.* To visualize the microbial log ratio signatures, we
263 constructed undirected graphs connecting the key taxa (vertices/nodes) by edges representing the
264 formation of a ratio between two taxa with edge weight corresponding to the between-group
265 Kruskal-Wallis H-statistic. While the full log ratio structure is directed in distinguishing
266 numerators from denominators, directedness in the visualizations used here does not
267 fundamentally change our interpretation. Graphs were visualized using Gephi⁴⁷ and R-igraph.⁴⁸
268

269 *Multivariate statistical test for microbial signals.* To confirm associations between microbial log
270 ratio signatures and Sex/Exposure group multivariate hypothesis testing was done using
271 permutational multivariate analysis of variation⁴⁹ and implemented using the R vegan package.⁴³
272 Unsupervised lower-dimensional projections of samples and group centroids were done using
273 principal coordinate analysis (PCoA) and were implemented using the R stats package.
274

275 *Partial Least Squares Discriminate Analysis.* We utilized partial least squares discriminate
276 analysis (PLS-DA),^{50,51} a versatile multivariate statistical regression technique, to model and
277 understand the relationship between Sex/Exposure group to their microbial signatures. Shown to
278 have reliable performance on compositional and genomic datasets,^{52,53} PLS-DA models perform
279 classification, inference, and are inherently linear thus offering improved model interpretability.
280 We specified a priori the number of PLS-DA components (ncomp) as follows: for the between
281 Sex nasal microbial signature, ncomp = 1; for the between Exposure group nasal microbial
282 signature, ncomp = 2. Model fitting was done using the R caret⁵⁴ *plsda* function, with latent
283 space projections and loadings extracted from the final models fit using all samples using R
284 caret.⁵⁴ PLS-DA biplots were created by scaling and superimposing the loading vectors onto the
285 score coordinates extracted from the final fitted model. PLS-DA biplots were visualized using
286 the R ggplot2 package.⁵⁵
287

288 *Receiver operating characteristic curve analysis and PLS-DA performance metric.* To
289 understand how well the binary PLS-DA models discriminate between Sex using the nasal
290 microbiome signature, we utilized the area under the receiver operating characteristic metric,
291 AUC, which represents the probability that a randomly selected instance of class 1 will be ranked
292 higher than a randomly selected instance of class 2.⁵⁶ Additionally, to understand the
293 discriminatory potential of the ternary PLS-DA Exposure group models, the multi-class AUC
294 metric was used. The multi-class AUC generalizes binary AUC through pairwise class AUC
295 averaging and has the useful property of being independent of cost and priors as in AUC while
296 having a similar interpretation to misclassification rate.⁵⁷ AUC metrics were estimated using
297 repeated k-fold cross-validation.⁵⁸ The R pROC package⁵⁹ was used to compute all AUC
298 metrics. ROC curves, which graph the false positive and true positive rate of a classifier over a
299 range of thresholds, were computed using the R pROC package⁵⁹ and visualized using the R
300 ggplot2 package.⁵⁵

301
302 *NLF mediator and microbiome data integration.* We define the nasal lavage data matrix, $\mathbf{L} \in$
303 $\mathbb{R}^{n \times f}$, where $n = 66$ samples and $f = 7$ mediators. Treating the data as relative such that sample-

wise absolute concentrations in our study are considered unimportant (**Figure S3A**), zeroes were imputed after applying the closure operator to \mathbf{L} as described in our compositional data analysis methods. From this, we define $\mathbf{L}' \in \mathbb{R}^{n \times k}$, with $k = 21$, to include all pairwise log ratios from \mathbf{L} . To remove uninformative NLF mediators, we computed the differential compositional variation (DCV) score³² and assigned each NLF mediator log ratio a score by averaging the within-fold DCV score using 20 repeats of 10-fold cross-validation. NLF log ratios with a DCV score < 0 were considered uninformative and were removed (**Figure S3B**). From this ' was reduced to $\hat{\mathbf{L}} \in \mathbb{R}^{n \times k}$ where $k=4$ (**Figure S3C**) log ratios. To test for univariate associations between NLF mediator log ratios and Exposure group the Kruskal-Wallis test was applied followed by pairwise Wilcoxon rank-sum testing if $\alpha < 0.05$. The nasal microbiome signal was obtained by applying the SelEnergyPerm method to \mathbf{M} to get $\hat{\mathbf{M}} \in \mathbb{R}^{n \times r}$ where $n = 62$ and $r = 9$ log ratios.

Concatenating these data, we define the integrated NLF mediator and nasal microbiome matrix as $\mathbf{D} \in \mathbb{R}^{n \times f}$ where $n = 61$ (6 samples were removed due to either missing nasal microbiome or NLF data) and $f = 13$ (4-nasal lavage and 9 microbiome log-ratio features). Exposure group discrimination was estimated separately for each of $\hat{\mathbf{L}}$, $\hat{\mathbf{M}}$, and \mathbf{D} using multi-class AUC from 50 repeats of 10-fold cross-validation using 2-component PLS-DA models. Multi-class AUC estimates using $\hat{\mathbf{L}}$, $\hat{\mathbf{M}}$, and \mathbf{D} were compared between groups using the non-parametric Wilcoxon rank-sum test.

Nasal NLF mediator and microbiome association analysis

A final 2-component PLS-DA model to discriminate between exposure groups was fit to $\hat{\mathbf{M}}$. Using dimensionality reduction inherent to PLS-DA, the first PLS-DA component (explaining the most variation) was extracted as a latent variable for further analysis. Pearson's correlation coefficients (PCC) and subsequent p-values were computed between the first PLS-DA component and \mathbf{L}'' represent the reduced nasal microbiome exposure group signature. PCC p-values, adjusted for multiple comparisons (q-value) using the Benjamini-Hochberg (BH) correction,⁶⁰ were considered significant if $q \leq 0.10$. These analyses were carried out using the R stats and caret packages.

Between Exposure group Correlation analysis. Partitioning the samples of \mathbf{D} into 3 matrices based on exposure group (nonsmokers, e-cig users, or smokers), we calculate all pairwise PCC and p-values between features for each group. We also report q-values after adjusting for multiple comparisons within each group using the BH method. Correlations were considered significant if $q \leq 0.10$. Significant PCC within each subject were then aggregated across all exposure groups and visualized as a graph using the R igraph package.⁴⁸

Confidence Intervals and univariate statistical test for log ratios. Log ratio 95% confidence interval estimates were calculated by

$$CI_i = \bar{x}_i \pm 1.96 \frac{s_i}{\sqrt{n}}$$

where for the i th log ratio, \bar{x}_i = sample mean, s_i = sample standard deviation and n =number samples. Log ratios with confidence intervals bounds that do not include 0 are interpreted as enriched on average for the numerator if $\bar{x} > 0$ or denominator if $\bar{x} < 0$. The Kruskal-Wallis

349 and Wilcoxon rank-sum test were used for univariate comparisons of log ratios between Sex or
350 Exposure groups. Moreover, p-values were adjusted for multiple comparisons using the BH
351 correction using the R stats library and are reported as q-values.

352

353 Results

354

355 Subject Demographics

356

357 Demographic, questionnaire, and smoking/vaping diary data are summarized in **Table 1**. The
358 study cohort was comprised of 30% nonsmokers ($n = 20$), 42% e-cigarette users ($n = 28$), and
359 28% smokers ($n = 19$) with at least $n = 8$ per sex within each exposure group. E-cigarette users
360 were significantly younger (26.39 ± 1.44) than nonsmokers (30.75 ± 1.32) and smokers ($31.89 \pm$
361 1.91) ($p < 0.05$). BMI did not differ significantly between the exposure groups. Questionnaires
362 and smoking/vaping diaries were completed for 95% (19/20) of nonsmokers and 100% of e-
363 cigarette users and smokers. However, there was variability in the completeness of diaries filled
364 out by e-cigarette users, particularly for the e-cigarette use parameters (mL/day, puffs/day,
365 nicotine concentration, flavor, device). Cigarette users smoked an average of 12.68 ± 0.96
366 cigarettes per day, whereas 25% (7/28) of e-cigarette users smoked a cigarette during the diary
367 period with an average of 0.14 ± 0.07 cigarettes per day, while 13 e-cigarette users reported puffs
368 per day and 16 reported mL e-liquid/day and e-liquid nicotine concentration in mg/mL. These e-
369 cigarette users averaged 53.90 ± 16.54 puffs/day, 3.60 ± 0.70 mL of e-liquid, and 19.43 ± 4.92
370 mg/mL nicotine in e-liquids. One smoker reported vaping on one day of the diary, which is the
371 reason for the non-zero values for e-cigarette use parameters in the smoker category.

372 Nonsmokers did not report previous cigarette smoking or marijuana use, whereas 79% (22/28) of
373 e-cigarette users were former cigarette smokers, while 14% (4/28) of e-cigarette users and 21%
374 (4/19) of smokers reported marijuana use in their diaries. Cotinine, a metabolite of nicotine, was
375 not detectable in the serum of nonsmokers and was significantly elevated in the serum of e-
376 cigarette users (127.99 ± 15.42) and smokers (170.16 ± 21.41) in comparison with nonsmokers
377 ($p < 0.0001$), as expected.

378

379 Nasal Microbiome Characteristics

380

381 The 4677 OTUs included in the dataset represented OTUs from 19 unique phyla and 225 unique
382 genera. The top four most abundant phyla by average relative abundance across all samples were
383 *Actinobacteria* (50.2%), *Firmicutes* (36%), *Proteobacteria* (12.0%), and *Bacteroidetes* (1.6%).
384 The top six most abundant genera by average relative abundance across all samples were
385 *Corynebacterium* (40.7%), *Staphylococcus* (19.9%), *Propionibacterium* (11.8%), *Alliococcus*
386 (8.5%), *Moraxella* (5.3%), and *Streptococcus* (4.2%). This microbial composition is similar to
387 previously reported studies of the nasal microbiome.^{61,62} These data are summarized in **Figure 1**,
388 where relative abundances by exposure group and sex are plotted for the most highly abundant
389 phyla and genera.

390

391 Alpha Diversity

392

393 To determine whether there are differences in alpha diversity between the nasal microbiomes of
394 smokers, nonsmokers, and e-cigarette users, we calculated alpha diversity indices (Observed,

395 Chao1, ACE, Shannon, Simpson, Fisher) using phyloseq.⁶³ We did not find any statistically
396 significant differences between the exposure groups for any measure of alpha diversity; however,
397 we did observe a non-significant trend of increased alpha diversity in smokers (**Figures 2A and**
398 **2B**). Because our group and others have previously observed sex differences in respiratory
399 mucosal immune responses^{64,65} we also tested whether alpha diversity was significantly different
400 between male and female subjects. We found that both the Shannon and Simpson indices were
401 significantly higher in males than females ($p = 0.021$ and $p = 0.0078$, respectively) (**Figures 2C**
402 and **2D**). We then tested for the interaction between sex and exposure group and found that sex
403 was a significant source of observed variation ($p = 0.0286$ for Shannon; $p = 0.0102$ for Simpson),
404 while exposure group was not. When the data were stratified by exposure group, the only male-
405 female comparison that remained significant was in the e-cigarette user group ($p = 0.0361$ for
406 Shannon; $p = 0.0124$ for Simpson) (**Figures 2E and 2F**). These results suggest that sex is an
407 important biological variable to consider in studies of the nasal microbiome.

408

409 *Compositional Difference of the Nasal Microbiome by Sex*

410

411 Because we observed distinctions in alpha diversity between sexes, we next tested whether there
412 were significant compositional differences between the sexes and to identify specific genera
413 capable of explaining these dissimilarities. Given challenges presented by sparse, compositional
414 16S rRNA sequencing data combined with high-dimensionality (genera = 255) and small sample
415 size ($n=62$), we leveraged the SelEnergyPerm³² method to identify a robust signature of nasal
416 microbiome taxa (among sparse noisy data) capable of explaining compositional differences
417 between sexes.

418

419 By applying this method, we discovered (beyond random noise) a subset of genera ($g = 6$)
420 capable of maximizing the energy distance between male and female samples ($p = 0.0123$,
421 **Figure S1A**). This microbial signature was comprised of four log ratios between *Rhodococcus*,
422 *Finegoldia*, *Sneathia*, *Abiotrophia*, *Tannerella*, and *Yaniella* genera (**Figure 3A**). Using the
423 identified log ratio signature, PERMANOVA analysis (pseudo- $F = 16.586$, $p = 0.0002$, **Figure**
424 **3B**) also confirmed the existence of differences in the nasal microbiome composition between
425 sex. Analysis of individual taxa log ratios between sexes demonstrated important nasal
426 microbiome compositional differences (**Figure 3C**). In female samples, *Yaniella* was more
427 abundant on average than *Rhodococcus* and *Tannerella*, while the reverse was true for males. In
428 male samples, *Abiotrophia* was more abundant on average than *Sneathia*, while the opposite was
429 true for females. Finally, in both males and females, *Finegoldia* was observed to be more
430 abundant than *Yaniella*, however, *Finegoldia* was significantly more enriched relative to *Yaniella*
431 in males compared to females.

432

433 Next, we analyzed the microbial signature as a whole using Partial Least Squares Discriminate
434 Analysis (PLS-DA) with a single component to predict sex. Using 20 repeats of 10-fold cross-
435 validation, the average area under the receiver operating characteristic curve (AUC) for
436 predicting sex given the reduced microbial signature was 0.862 (95% CI 0.842 – 0.883, **Figure**
437 **3D**). With strong cross-validated predictive performance, a final PLS-DA model was trained on
438 all samples ($n=62$). Scores from the single PLS-DA component indicated strong separation
439 between sexes (**Figure 3E**). The PLS-DA loading plot (**Figure 3F**), which shows how each log
440 ratio contributes to the final score, demonstrates key relationships between taxa log ratios.

441 Increased abundance of *Abiotrophia* and *Finegoldia* (in log ratios where they appear) were
442 characteristic of males, and increased abundance of *Yaniella* was associated with females.
443 Overall, these findings indicate there exists a compositionally distinct taxa subset that differs
444 strongly in the nasal microbiomes of males and females. Therefore, controlling for sex
445 differences present in the nasal microbiome is important in further analysis.
446

447 *Compositional Difference of the Nasal Microbiome by Exposure group*

449 We next examined whether there were distinct nasal microbiome compositions between
450 exposure groups (e-cigarette users: n = 24; smokers: n=19; nonsmokers: n=19; See Methods and
451 **Table 1**). Taking into account nasal microbiome sex differences and applying SelEnergyPerm,
452 we identified a subset of genera ($g = 12$) important for explaining key nasal microbiome
453 alterations between exposure groups ($p = 0.032$, **Figure S1B**). This microbial signature
454 comprised nine log ratios (edges) between 12 key genera (nodes) (**Figure 4A**). PERMANOVA
455 analysis (pseudo- $F = 8.4889$, $p = 0.0002$, **Figure 4B**) confirmed differences in nasal microbiome
456 composition between exposure groups given the microbial signature of 9 log ratios.
457

458 Individual analyses of log ratios elucidated specific compositional differences between exposure
459 groups (**Figure 4C**). In e-cigarette users, *Lactobacillus* taxa were significantly more abundant
460 relative to *Bacillus* taxa, while in smokers and nonsmokers, these taxa presented in similar
461 proportions, suggesting an enrichment of *Lactobacillus* among e-cigarette users. E-cigarette
462 users' nasal microbiomes also contained significantly more *Staphylococcus* relative to *Bacillus*
463 than what was observed in nasal microbiomes of both smokers ($q = 0.0097$) and nonsmokers ($q =$
464 0.0031). In smokers, *Maccrocus* genera were significantly more abundant on average relative to
465 *Hymenobacter*, *Mycobacterium*, *Varibaculum*, and *Rhodococcus*, suggesting that smoking may
466 enrich *Macrococcus* taxa populations in the nasal passage. Additionally, smoker nasal
467 microbiomes contained more *Hymenobacter* relative to *Moryella*, whereas the opposite was true
468 for nonsmokers, both in contrast to e-cigarette users, which maintained on average equal
469 amounts of both genera. In nonsmokers, *Lautropia* taxa were significantly more abundant
470 relative to *Bulleidia*, but this was not observed in smokers and e-cigarette users.
471

472 To understand how taxa log ratios work together to discriminate between exposure groups, PLS-
473 DA was used with 20 repeats of 10-fold cross-validation (**Figure 4D**). The estimated multi-
474 classification AUC was 0.851 (95% CI 0.835 – 0.866) suggesting excellent exposure group
475 discrimination. Pairwise examination of exposure group classifications shows strong differences
476 between the nasal microbiomes of nonsmokers/e-cigarette users (AUC = 0.895: 95% CI 0.874 –
477 0.915) and smokers/e-cigarette users (AUC = 0.893: 95% CI 0.873 – 0.913), with weaker yet
478 distinct differences between smokers/nonsmokers (AUC = 0.803: 95% CI 0.773 – 0.833)
479 (**Figure 4D**). The relative importance of taxa log ratios for discriminating between exposure
480 groups was computed using a final PLS-DA model fit using all samples ($n=62$). The log ratio
481 between *Macrococcus* relative to *Hymenobacter* was found to be most important for classifying
482 samples as smoker (least important for e-cigarette user classification), and the log ratio between
483 *Bacillus* taxa relative to taxa from the *Micrococcaceae* family was most important for samples to
484 be classified as e-cigarette users (least important to be classified as smokers). (**Figure 4E**).
485 Interestingly, inspection of relative log ratio importance data failed to uncover log ratios
486 disproportionately important for nonsmokers. This observation suggests smoking and e-cigarette

487 use recognizably alter the nasal microbiome in otherwise healthy adults. Overall, analysis of the
488 taxa log ratios signature suggests alterations in *Macrococcus* and *Bacillus* genera are important
489 for distinguishing between these exposure groups.

490

491 *Differences in NLF mediator Expression Patterns Between Exposure groups*

492

493 Because smoking and e-cigarette use were associated with distinct changes in the nasal
494 microbiome, we next explored if there was altered expression of innate immune response
495 mediators in the exposure groups. Accounting for differences in absolute concentration ([Figure S3A](#)) and subsequently applying differential compositional variation scoring³² (See Methods,
496 [Figure S3B](#)), we identified four log ratios among NLF mediators that showed strong intergroup
497 variability ([Figure S3C](#)). These ratios comprised the following NLF mediators: IL-8, DEFB4A-
498 2, neutrophil elastase, IgA, and lactoferrin. Kruskal-Wallis one-way testing ([Figure S3D](#)) of
499 each log ratio suggest there exist intergroup differences in NLF mediator expression formed
500 between the concentrations of neutrophil elastase relative to IL-8 ($H = 6.4417$; $p = 0.0399$; $q =$
501 0.0798) and lactoferrin relative to IL-8 ($H = 8.2080$; $p = 0.0165$; FDR = 0.0660). There were no
502 significant differences between exposure groups among log ratios formed by IgA relative to IL-8
503 or DEFB4A-2 relative to neutrophil elastase. However, multivariate analysis with
504 PERMANOVA (pseudo- $F = 3.7678$, $p = 0.0030$) using the four key log ratios confirmed there
505 were differences in NLF mediator expression patterns between exposure groups when considered
506 together. To better understand which groups were different, we applied PLS-DA. Training a
507 PLS-DA model with the NLF mediator expression patterns revealed the strongest between-
508 subject-group discrimination to be among Smokers and Nonsmokers (AUROC = 0.8230, 95%CI
509 0.7920-0.8530, [Figure S3E](#)). Notably, e-cigarette users' NLF mediators were weakly
510 distinguishable from nonsmokers (AUROC = 0.6720, 95%CI 0.6350-0.7100, [Figure S3E](#)) but
511 more discernible from smokers (AUROC = 0.7480, 95%CI 0.7130-0.7820, [Figure S3E](#)).
512 Together, these results suggest that the expression of NLF mediators in smokers was distinct
513 from that of e-cigarette users and healthy adults.

514

515 *Integration of NLF mediators and nasal microbiome composition improves exposure group 516 discrimination*

517

518 Finally, we aimed to understand if alterations in NLF mediator expression are associated with
519 nasal microbiome dysbiosis resulting from smoking or e-cigarette use. To this end, we first
520 estimated the discriminatory AUROC of a 2-component PLS-DA model fit on log ratios from
521 NLF mediators ([Figures S2C - S3](#)), nasal microbiome ([Figures 4A – S4A](#)), or both nasal
522 microbiome and NLF mediators ([Figure 5A](#)). When compared to individual signatures,
523 improved discriminatory AUROC ([Figure 5B](#)) was observed when PLS-DA models were fit
524 using the combined nasal microbiome and NLF mediator signatures. Therefore, with established
525 synergy between mediator expression and nasal microbiome composition in discriminating
526 between exposure groups, we next examined if correlations were present between the two.

527

528 *Association between altered NLF mediator expression and nasal microbiome dysbiosis*

529

530 Using the first PLS-DA component of the nasal microbiome signature, we found significant
531 correlations with NLF mediator expression, showing an association between the nasal

533 microbiome composition and NLF mediator expression (**Figure 5C**). Examination of the
534 location of samples by exposure group projected along the first PLS-DA component show
535 important projective distinctions between smokers (on average negative projections) and both e-
536 cigarette users and nonsmokers (on average positive projections) (**Figure S4B**). Given this, these
537 correlations suggest nasal microbiome dysbiosis caused by cigarette smoke exposure is
538 associated with increased expression of IL-8 relative to neutrophil elastase, Total IgA, and
539 lactoferrin (**Figure 5C**). Moreover, the loadings along the first PLS-DA component (**Figure**
540 **S4C**) show log ratios with higher abundance of *Macrococcus* as being the most important
541 contributor to negative projections. Combined, these data propound an important link between
542 dysbiosis in *Macrococcus* communities within the nasal microbiome and NLF IL-8 expression.
543

544 *Microbial functional and mediator expression differences between exposure groups*

545
546 Correlation analysis of the combined NLF mediator expression and nasal microbiome signature
547 reveal distinct correlation patterns within exposure groups suggesting distinct functional
548 differences (**Figures 5D**). Most notably, a significant negative correlation between log ratios
549 formed by *Hymenobacter/Moryella* and *Macrococcus/Hymenobacter* was observed only in the
550 nonsmoker group. This negative correlation highlights a possible role of *Hymenobacter*, in that it
551 appears to be important for maintaining a healthy balance of *Macrococcus* and *Moryella*. In the
552 e-cigarette and smoking groups, we observed a significant positive correlation between the log
553 ratios formed by IgA/IL-8 and Lactoferrin/IL-8. Analysis of this correlation pattern reveals that
554 increased expression of IL-8 in these groups may come at the expense of decreased expression of
555 IgA and lactoferrin or vice versa. We also observed a significant negative correlation between
556 the log ratios formed by Neutrophil Elastase/IL-8 and DEFB4A-2/Neutrophil Elastase in the e-
557 cigarette and smoking groups. These strong negative correlations show that increased expression
558 of IL-8 and DEFB4A-2 subsequently results in decreased expression of neutrophil elastase. The
559 final significant correlation pattern observed was in smokers only and consisted of four
560 positively correlated log ratios formed by *Macrococcus* relative to *Hymenobacter*,
561 *Mycobacterium*, *Varibaculum*, and *Rhodococcus* (**Figure 5D**). Relatively interpreting these
562 correlations between log ratios suggests that as *Macrococcus* becomes more abundant (among
563 these ratios) the abundance of *Hymenobacter*, *Mycobacterium*, *Varibaculum*, and *Rhodococcus*
564 decreases. This suggests that cigarette smoke exposure may produce favorable colonization
565 conditions for *Macrococcus* genera which subsequently reduces the abundance of
566 *Hymenobacter*, *Mycobacterium*, *Varibaculum*, and *Rhodococcus*.

567 From these analyses, our results demonstrate there exists a strong association between altered
568 NLF mediator expression and nasal microbiome dysbiosis. Our findings indicate nasal
569 microbiome dysbiosis from smoking results in the simultaneous increase in IL-8 expression and
570 *Macrococcus* abundance. Additionally, variations in the correlation networks among e-cigarette
571 users and smokers, while similar, were distinct from nonsmokers, suggesting functional
572 differences at the microbial and mediator levels between exposure groups.

573
574 **Discussion**

575
576 Despite the growing body of research showing that e-cigarette use can disrupt the
577 respiratory immune system, no studies to date have assessed the effects of e-cigarettes on the

579 respiratory microbiome and host-microbiota interactions. In this study, after adjusting for sex
580 differences, we found that e-cigarette users, smokers, and nonsmokers have unique nasal
581 microbiomes, with differences driven by the relationships between a subset of key taxa. We also
582 found a subset of immune mediators that had distinct relationships between each other in the
583 different exposure groups. Importantly, we found a link between nasal microbiome dysbiosis and
584 soluble immune mediator networks.

585 A fundamental feature of our study is that we detected microbial signatures from the
586 nasal microbiome that explained differences between sex and exposure groups using the novel
587 SelEnergyPerm computational method. This method directly accounts for the sparse, high-
588 dimensional and compositional nature of the 16S relative abundance data. Additionally,
589 SelEnergyPerm identifies subsets of robust log ratios between taxa, as opposed to analyzing taxa
590 relative abundance alone, yielding higher statistical power in the sparse association setting with
591 low-sample-size compositional data.³² Most importantly, traditional statistical techniques such
592 as PERMANOVA, ANOSIM, and ANCOM alone were unable to detect these sparse
593 associations within the high-dimensional nasal microbiome feature space. Further, our
594 parsimonious yet statistically significant signatures were then integrated with NLF mediators
595 where we were then able to uncover novel interactions between a taxa subset within the nasal
596 microbiome and the NLF mediators in response to exposure to cigarette or e-cigarette aerosol.

597 We observed that there were relationships between a subset of taxa that were important in
598 separating the microbial communities of smokers, nonsmokers, and e-cigarette users ([Figure 4](#)).
599 Only a few studies have previously compared the nasal microbiome of smokers and
600 nonsmokers.^{23,66} Charlson et al. found specific bacteria genera that were differentially abundant
601 in smokers and that some genera belonging to the phylum *Firmicutes* were important in
602 distinguishing smokers from nonsmokers.²³ Other studies did not find any significant differences
603 in diversity measures or relative taxa abundance between smokers and nonsmokers.⁶⁶ In our
604 study, which focused on the composition of the nasal microbiome and ratios between taxa rather
605 than relative abundance of individual taxa, we found that alterations in *Macrococcus* and
606 *Bacillus* genera are important for distinguishing between exposure groups. Our data also suggest
607 an enrichment of *Lactobacillus* and *Staphylococcus* relative to *Bacillus* in e-cigarette users and
608 enrichment of *Macrococcus* relative to *Hymenobacter*, *Mycobacterium*, *Varibaculum*, and
609 *Rhodococcus* in smokers. A shift from *Lactobacillus* to *Bacillus* in the lung microbiome has been
610 previously demonstrated in response to influenza A infection and increases in anaerobic bacteria,
611 such as *Lactobacillus*, have been associated with chronic rhinosinusitis.⁶¹ Furthermore, *Bacillus*
612 have been shown to produce antimicrobials against *S. aureus*,⁶⁷ indicating that the patterns we
613 have observed may be directly linked to specific interactions between taxa. An increase in
614 *Staphylococcus* relative to *Bacillus* in e-cigarette users is also notable due to the role of species
615 such as *Staphylococcus aureus*, which is carried normally by about 30% of people and is also
616 considered to be a potential pathogen of the skin and mucosal surfaces.^{68,69} Our data provide
617 evidence that e-cigarette and smoker nasal microbiomes are distinctly shifted from nonsmokers.
618 Importantly, we also observed that different subsets of taxa were important in separating e-
619 cigarette users and smokers, rather than effects on a continuum from nonsmokers to e-cigarette
620 users to smokers, highlighting the concept that the effects of e-cigarettes are likely unique from
621 those of smokers, even though they are commonly directly compared.

622 We also measured concentrations of mediators of host-microbiota interactions in nasal
623 lavage fluid to determine whether the changes in the nasal microbiome in different exposure
624 groups are potentially caused by direct effects on the microbiome, mediated by changes in the

host immune system, or both. Our data indicate that the expression of immune mediators in nasal lavage fluid samples differed among exposure groups and was driven by shifts in neutrophil elastase and lactoferrin relative to IL-8. Neutrophil elastase and IL-8 are associated with inflammation and neutrophil recruitment, while lactoferrin is an antimicrobial protein primarily produced by epithelial cells and has a wide array of functions, including antioxidant and immune-modulating properties.⁷⁰ Our results suggest that e-cigarette users and smokers may have altered immune mediator milieu, indicating a shift away from immune homeostasis and towards increased inflammation and neutrophil recruitment. This shift could be partially driving observed differences in the nasal microbiome.

Our data indicate that both e-cigarette users and smokers have altered nasal microbial communities and relationships between markers of innate immune response, which could imply that they are at increased susceptibility to respiratory infections and/or that they exist in a state of inflammation and altered immune response. We also uncovered interactions of key immune mediators with the host and microbiota, such as IL-8, neutrophil elastase, and lactoferrin, that are also disrupted by e-cigarette and cigarette use. The microbial shifts we observed in association with e-cigarette and cigarette use could be driven by changes in the microenvironment, such as temperature, pH, free radical formation, and availability of metabolic substrates (e.g. sugars) that could then alter the fitness of different bacteria in the nasal microbial community. The shifts we observed could also be mediated through direct effects on respiratory host defense function, inflammation, and/or specific microbes. Multiple processes are likely at play, but our novel findings on the effects of e-cigarettes on the nasal microbiome add to the growing body of literature demonstrating that e-cigarettes are not without health effects and that they should be more thoroughly investigated for inhalational toxicity.

Because sex differences in the human immune system and its response to respiratory disease and toxicant exposure have been observed previously,^{64,71} we also investigated whether there were sex differences in the nasal microbiomes of our subjects. We observed that the relationships between six genera were important in separating the nasal microbiomes of males and females (Figure 4A). Increased abundance of *Abiotrophia* and *Finegoldia* (in log ratios where they appear) were characteristic of males, and increased abundance of *Yaniella* was associated with Females. Many of these genera have been detected in previous studies of skin, oral, and/or respiratory microbiomes,^{23,61,72-76} but detailed information on the functions of these bacteria as part of the microbial community, as well as their impact on host health, are not available for all taxa. Although some of these genera, such as *Abiotrophia* and *Finegoldia* have been associated with disease- and exposure-driven alterations in the respiratory microbiome,^{23,61,72,73} we hypothesize that the observed sex difference is neither good nor bad; rather, it is reflective of a different baseline composition in males and females or altered microenvironments in males and females due to differences in toxicant metabolism rates or mechanisms of immune regulation.^{77,78} In other body sites, such as the gut, sex differences have been detected and have been attributed to a variety of factors, including sex hormone levels, pharmaceutical use, and diet.^{79,80} In mice, sex-related differences in gut microbiota were shown to impact pulmonary responses to ozone.⁶⁵ However, few studies have explored sex differences in the respiratory microbiome.⁸¹ In the studies that have analyzed data by sex, detection of sex differences is not consistent between studies and is typically not explored in-depth.^{62,68,82} Importantly for the data presented here, compositional differences in the nasal microbiomes of e-cigarette users, smokers, and nonsmokers were not apparent until sex was properly adjusted for,

670 further underscoring the importance of considering sex as a biological variable which
671 significantly modifies exposure effects and can substantially affect data interpretation.

672 Though our study reveals important community shifts in nasal microbiota and immune
673 mediators associated with e-cigarette and cigarette use as well as with sex, there are limitations
674 to our study. Our novel analysis approach, while properly accounting for the compositional
675 nature of the data, limits us in comparing our work to previous studies, which have been more
676 focused on specific taxa rather than ratios across the microbial community as a whole. As with
677 any study of human subjects, there is also inherent inter-subject variability that can interfere with
678 detection of differences between groups. In our e-cigarette user group, there was considerable
679 variability in factors that could impact the exposure subjects are receiving, including e-liquid
680 flavor, device, nicotine content, and frequency of use. The e-cigarette user group also includes
681 previous smokers and some marijuana use was reported in both smoker and e-cigarette user
682 questionnaires. These factors were included in our analysis and did not show a significant impact
683 on our overall findings due to the nature of the computational models we used. In future studies,
684 larger cohort sizes coupled with more extensive questionnaires could improve the ability to
685 detect which, if any, of these factors may be driving changes in microbiota composition and
686 would also increase power to detect overall changes and shifts in the nasal microbiomes of such
687 subjects given the compositional and sparse nature of 16S sequencing data.

688 As a whole, our results support and expand on the previously published notion that
689 exposure to inhaled toxicants, including tobacco products, can influence the respiratory
690 microbiome.^{23,83,84} The novel, robust computational approach in terms of pairwise log ratios that
691 we applied allowed us to uncover both exposure- and sex-dependent effects on nasal mucosal
692 host defense responses using straightforward, non-invasive sampling of the upper respiratory
693 tract of human subjects. Importantly, we were able to integrate 16S sequencing data with
694 expression of soluble immune mediators to understand interactions between the nasal
695 microbiome and host milieu by appropriately handling the sparse, compositional data generated
696 by 16S sequencing, accounting for inter-individual variability between subjects' mediator levels,
697 and selecting for features that were most important for separating classes, resulting in
698 interpretable, biologically meaningful results. Conventional analysis pipelines would have
699 limited our ability to integrate these two types of data and detect the exposure and sex-dependent
700 effects we observed, highlighting the importance of applying innovative computational methods
701 to address specific research questions and integrating multiple factors in understanding
702 biological outcomes of exposure and disease.

703
704 **Acknowledgments:** This research was funded by the National Institutes of Health
705 (NIH) Grant Nos. R01 HL139369, T32 ES007126, P50 HL120100, and F31 HL154758, by an
706 HHMI Gilliam Award (GT11504), and by a JSMF Complex Systems Scholar Award
707 (#220020315). The content is solely the responsibility of the authors and does not necessarily
708 represent the official views of any agency funding this research.

709
710 **Author Contributions:** I.J. and E.H. conceived the study and were in charge of overall direction
711 and planning. M.E.R., C.R., and I.J. contributed to clinical research operations, including the
712 collection and processing of samples and subject demographic data. B.Z. and M.W. performed
713 metagenomic sequencing, quality control, and analysis through OTU assignment. E.H.
714 performed experiments to measure proteins in nasal lavage fluid. A.H. led the remaining data

715 analysis with help from E.H. and feedback from P.J.M. and I.J.. E.H. and A.H. took the lead in
716 writing the manuscript. All authors provided feedback on and helped shape the final manuscript.
717

718 **Competing Interests Statement:** The authors report no competing interests.
719

720 **Data Availability:** Raw sequencing data is available under the SRA BioProject accession
721 number PRJNA746950. Processed OTU and NLF tables by exposure group and sex have been
722 deposited in the github repository:
723 https://github.com/andrew84830813/nasalMicrobiome_EcigSmoking/Data/
724

725 **Code accessibility**

726 All nasal microbiome analyses were done using version 4.0.0 of the R statistical programming
727 language. All input data, R script, and functions used in the analysis presented here can be
728 retrieved from the github repository:
729 https://github.com/andrew84830813/nasalMicrobiome_EcigSmoking.git
730

731 **Materials & Correspondence:** Ilona Jaspers, Ilona_jaspers@med.unc.edu
732
733

734
735
736
737
738

Table 1. Subject demographics. Reported values are mean \pm standard error. Groups were compared using the Steel Dwass method for non-parametric multiple comparisons. AA = African American. # $p < 0.05$ in comparison with nonsmokers and smokers. *** $p < 0.0001$ in comparison with nonsmokers.

	Nonsmokers	E-Cigarette Users	Smokers
n	20	28	19
Sex (Male/Female)	8/12	19/9	10/9
Race (White/AA/Asian/Other)	16/1/2/1	18/4/5/1	10/8/0/1
Age	30.75 ± 1.32	$26.39 \pm 1.44^{\#}$	31.89 ± 1.91
BMI	27.11 ± 1.31	30.07 ± 1.51	27.65 ± 1.43
Cigarettes/Day	0 ± 0	0.14 ± 0.07	12.68 ± 0.96
mL E-Liquid/Day	0 ± 0	3.60 ± 0.70	0.015 ± 0.015
E-Cigarette Puffs/Day	0 ± 0	53.90 ± 16.54	0.466 ± 0.414
E-Liquid Nicotine (mg/mL)	0 ± 0	19.43 ± 4.92	0.158 ± 0.158
Former Cigarette Smoker (Yes/No)	0/20	22/6	19/0
Marijuana Use (Yes/No)	0/20	4/24	4/15
Serum Cotinine (ng/mL)	0 ± 0	$127.99 \pm 15.42^{***}$	$170.16 \pm 21.41^{****}$

739
740
741

742
743

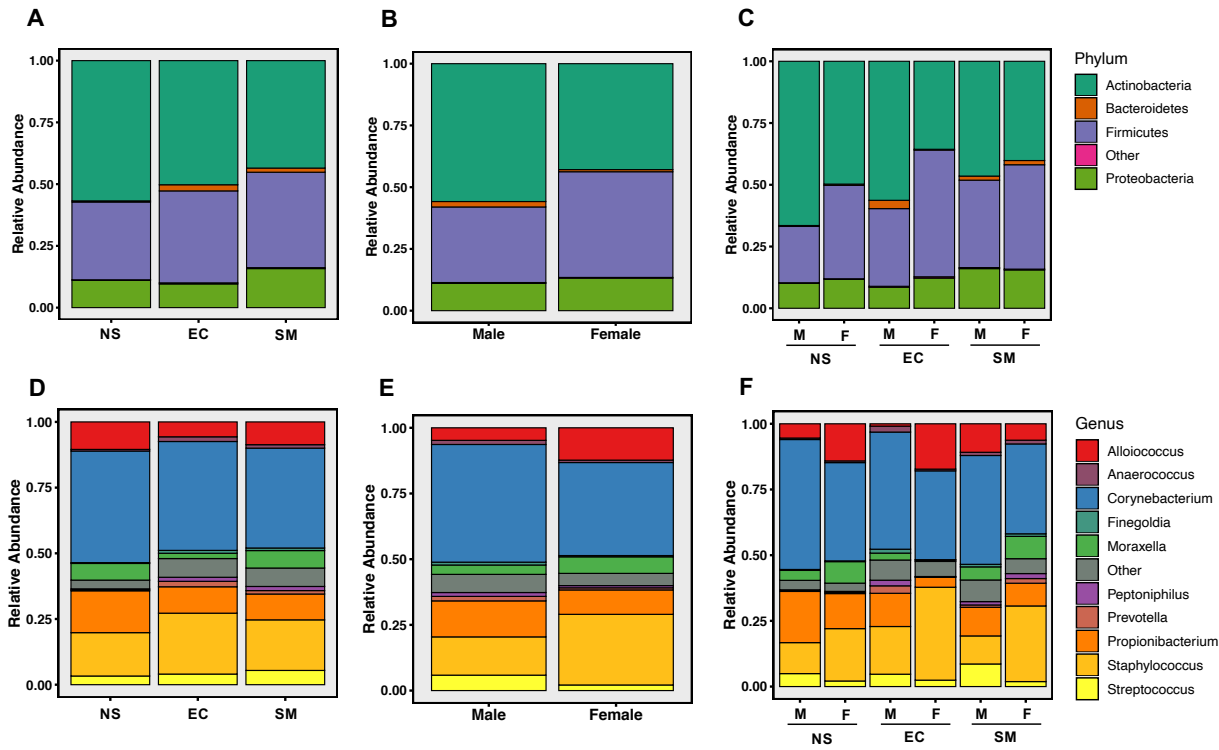


Figure 1. Average relative abundances of the top 4 phyla (A-C) and top 10 genera (D-E) plotted by exposure group (A, D), sex (B, E), and sex within exposure groups (C, F). NS = nonsmoker, EC = e-cigarette user, SM = smoker, M = male, F = female.

744
745
746
747

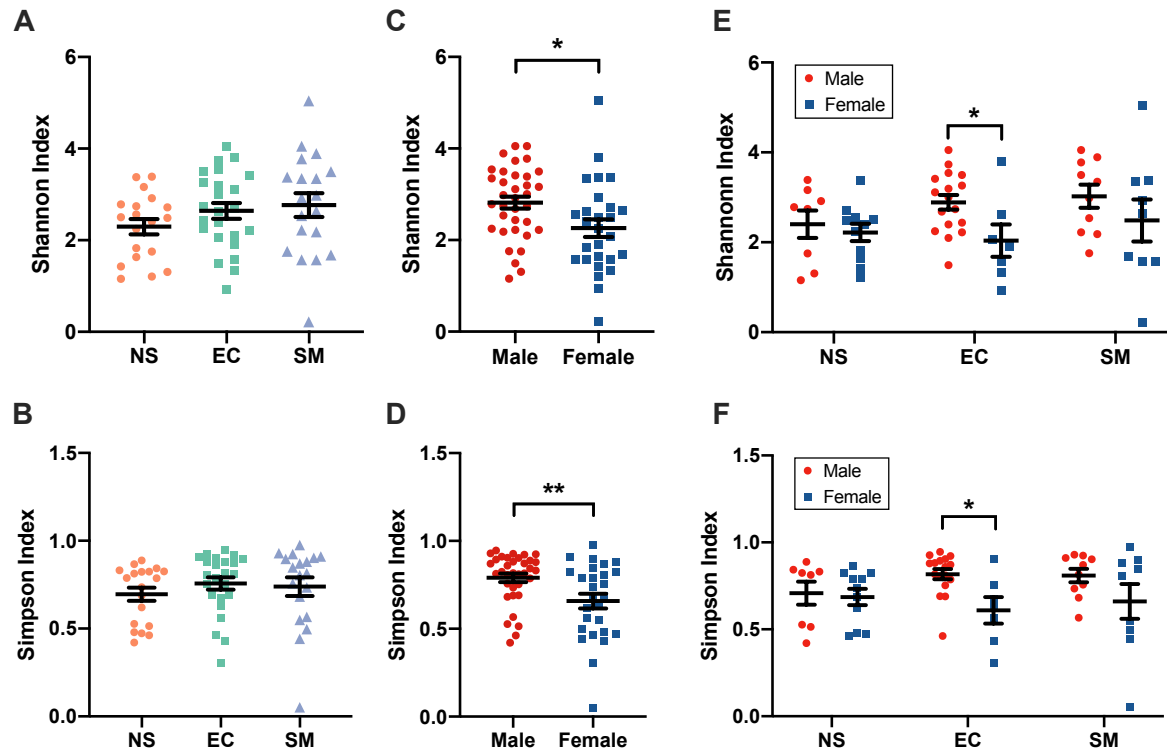


Figure 2. Shannon and Simpson indices of alpha diversity are significantly different between sexes, and this difference is most pronounced in e-cigarette users. The Shannon and Simpson indices for alpha diversity were calculated and plotted by exposure group (A, B), sex (C, D), and sex within exposure groups (E, F). NS = nonsmoker, EC = e-cigarette user, SM = smoker. Data are presented as mean \pm standard error. * $p < 0.05$, ** $p < 0.01$ by t-test (C), Kruskal-Wallis test (D), or two-way ANOVA with Fisher's LSD (E, F).

748
749
750
751
752
753
754
755
756
757
758
759
760
761
762
763

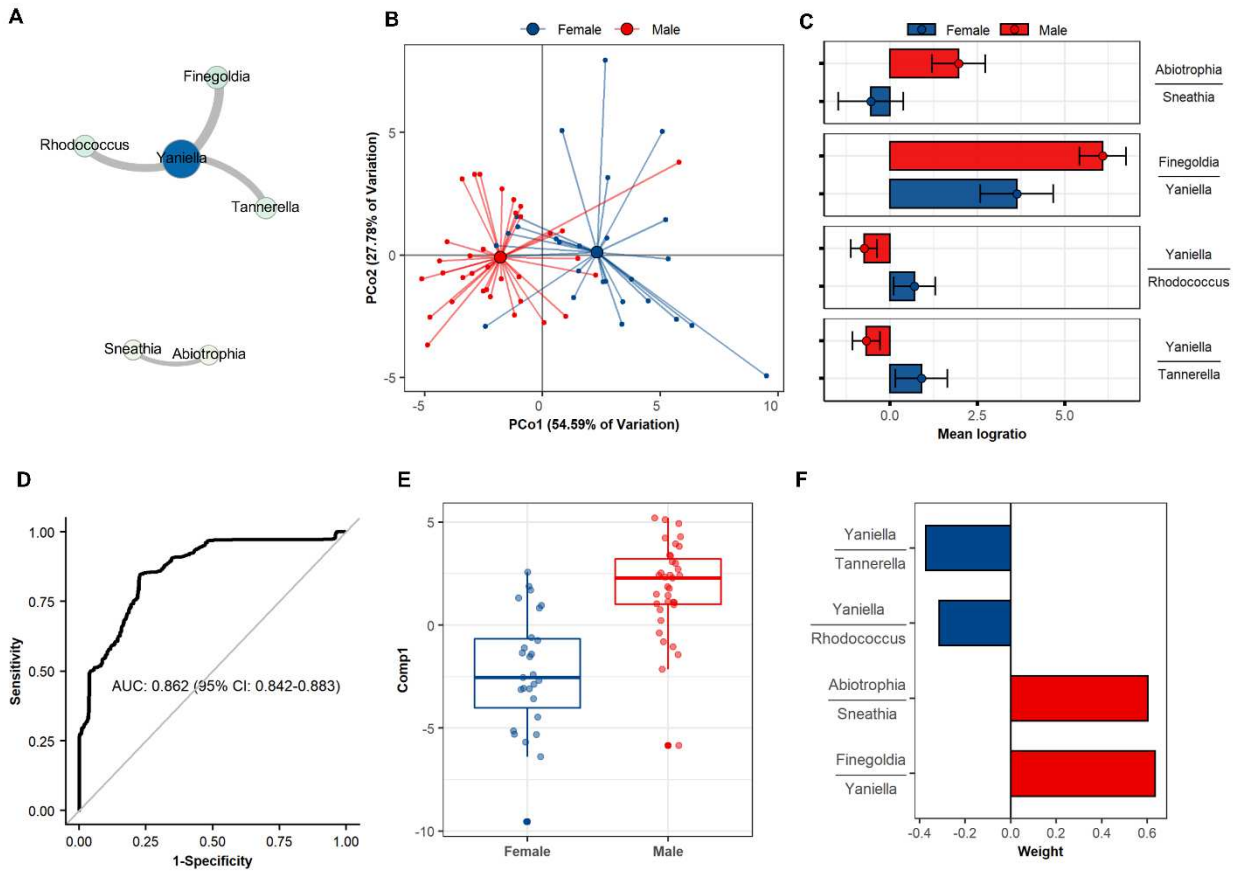


Figure 3 | Nasal microbiome differences between sexes (Males: n=35; Females: n=27). (A) Network representation of SelEnergyPerm ($p=0.0123$) derived genus aggregated taxa log ratio signature of nasal microbiome differences between sexes (Node = genera; edge = log ratio between taxa, Edge-weight = Kruskal Wallis H-statistic between sexes, Size/Color = node strength). (B) Principal coordinate analysis plot of nasal microbiome log ratio signature between sex explaining 82.37% of the total variation. (C) Univariate analysis of log ratio signature showing average depletion or enrichment of specific taxa log ratios between sexes. Error bars reflect 95% confidence intervals of the mean log-ratio value for males and females. (D) Receiver operating characteristics (ROC) curve displaying the area under the curve (AUC) predictive performance (20x10-fold cross-validation) of 1-component partial least squares discriminant analysis (PLS-DA) models trained on nasal microbiome signature between sexes. (E) PLS-DA scores plot of single discriminating component between sexes. Final PLS-DA model fit using all samples (n=62). (F) PLS-DA loadings plot showing contributions of each log ratio to final scores.

764
765
766
767
768
769
770

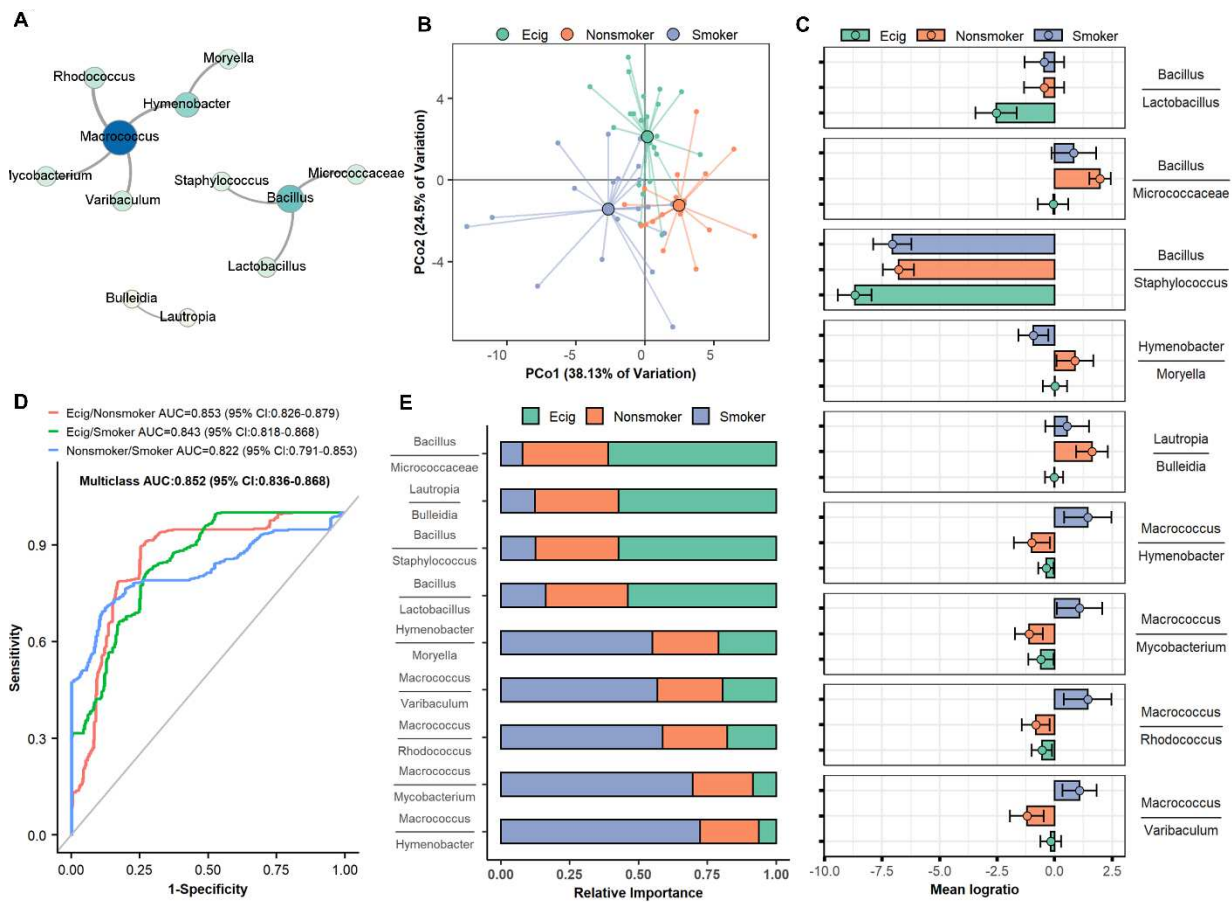


Figure 4 | Nasal microbiome differences between exposure groups (Ecig-users: $n=24$; Nonsmokers: $n=19$; and Smokers: $n=19$) adjusted for sex. (A) Network representation of SelEnergyPerm ($p=0.032$) derived genus aggregated taxa log ratio signature of nasal microbiome differences between exposure groups (Node = genera; edge = log ratio between taxa, Edge-weight = Kruskal Wallis H-statistic between sex, Size/Color = node strength). (B) Principal coordinate analysis plot of nasal microbiome log ratio signature between exposure groups explaining 62.63% of the total variation. (C) Univariate analysis of log ratio signature showing average depletion or enrichment of specific taxa log ratios between exposure groups. Error bars reflect 95% confidence intervals of the mean log-ratio value for each exposure group. (D) ROC curve displaying the multi-classification AUC for predicting exposure group (20x10-fold cross-validation) of 2-component PLS-DA models trained on nasal microbiome signature between exposure groups. (E) Relative importance of log ratios for distinguishing between exposure groups in PLS-DA model trained on all samples ($n=62$).

771
772
773
774
775
776
777
778

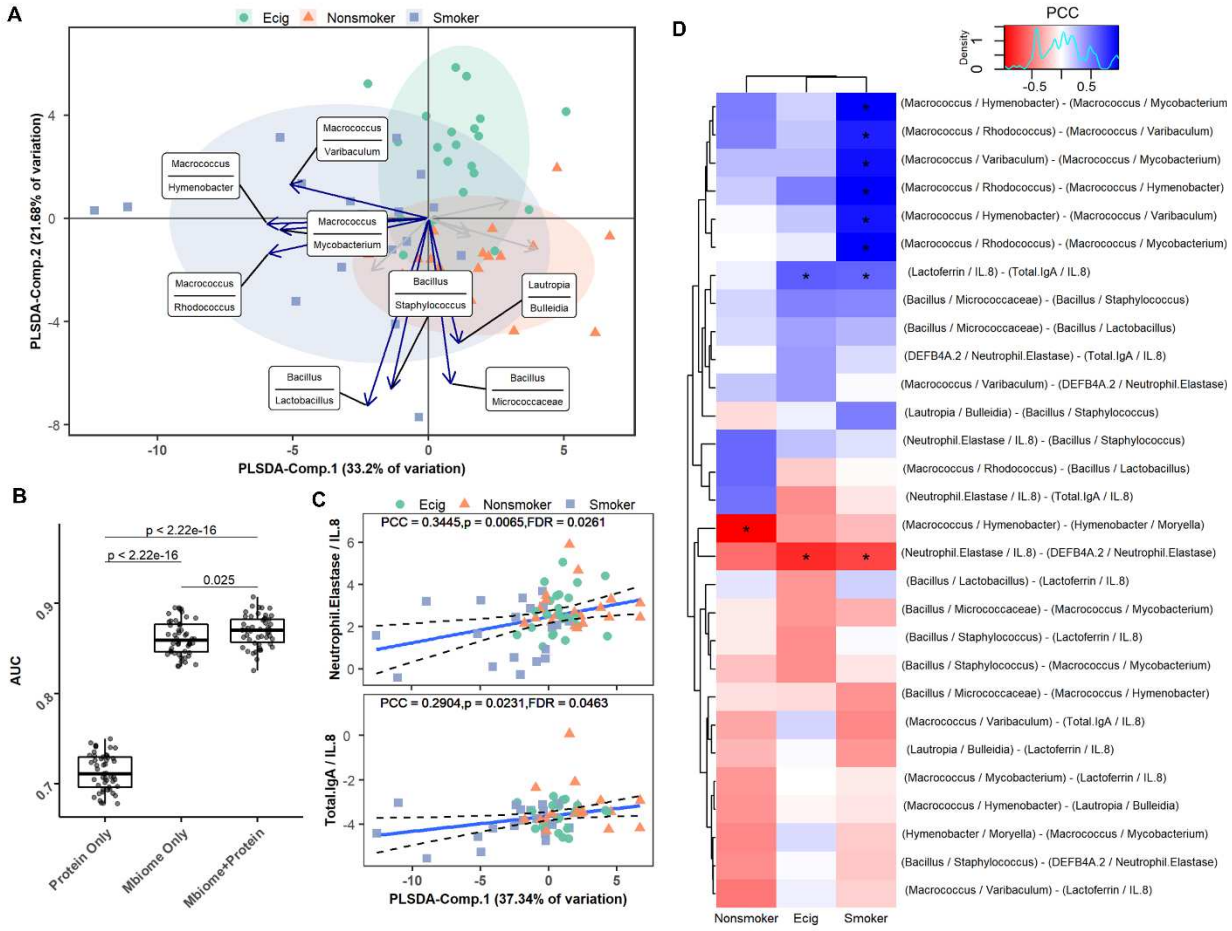


Figure 5 | Integrating data uncovers association between NLF mediators and nasal microbiome along with identifying distinct correlation patterns between exposure groups (Ecig-users: n=23; Non-smokers: n=19; and Smokers: n=19). (A) PLS-DA biplot of integrated NLF mediators and nasal microbiome (B) Box and whisker's plot comparing area under the receiver operating characteristic curve performance of 2-component PLS-DA model (50x10-fold cross-validation) using each data type alone or integrated. (C) Scatter plot showing correlations between log ratios formed between concentrations ($\mu\text{g/mL}$) of Lactoferrin, Neutrophil Elastase relative to IL-8 and the first PLS-DA component of the nasal microbiome. (D) Correlation heatmap showing Pearson's correlation coefficients (PCC) between and within the microbiome and protein log ratio signatures. (* indicates within group $q \leq 0.10$)

780 **References**

- 781 1 Wang, T., Asman, K., Gentzke, A. & al., e. Tobacco Product Use Among Adults — United
782 States, 2017. *MMWR Morb Mortal Wkly Rep* **67**, 1225–1232, doi:
783 <http://dx.doi.org/10.15585/mmwr.mm6744a2> (2017).
- 784 2 Leventhal, A. M. et al. Flavors of e-Cigarettes Used by Youths in the United States. *Jama*,
785 doi:10.1001/jama.2019.17968 (2019).
- 786 3 Wang, T. W. et al. E-cigarette Use Among Middle and High School Students - United
787 States, 2020. *MMWR Morb Mortal Wkly Rep* **69**, 1310-1312,
788 doi:10.15585/mmwr.mm6937e1 (2020).
- 789 4 Cullen, K. A. et al. e-Cigarette Use Among Youth in the United States, 2019. *Jama*,
790 doi:10.1001/jama.2019.18387 (2019).
- 791 5 Kiernan, E. et al. A Brief Overview of the National Outbreak of e-Cigarette, or Vaping,
792 Product Use-Associated Lung Injury and the Primary Causes. *Chest* **159**, 426-431,
793 doi:10.1016/j.chest.2020.07.068 (2021).
- 794 6 McAlinden, K. D. et al. COVID-19 and vaping: risk for increased susceptibility to SARS-
795 CoV-2 infection? *Eur Respir J* **56**, doi:10.1183/13993003.01645-2020 (2020).
- 796 7 Martin, E. M. et al. E-cigarette use results in suppression of immune and inflammatory-
797 response genes in nasal epithelial cells similar to cigarette smoke. *Am J Physiol Lung Cell
798 Mol Physiol* **311**, L135-144, doi:10.1152/ajplung.00170.2016 (2016).
- 799 8 Reidel, B. et al. E-Cigarette Use Causes a Unique Innate Immune Response in the Lung,
800 Involving Increased Neutrophilic Activation and Altered Mucin Secretion. *Am J Respir
801 Crit Care Med* **197**, 492-501, doi:10.1164/rccm.201708-1590OC (2018).
- 802 9 Clapp, P. W. et al. Flavored e-cigarette liquids and cinnamaldehyde impair respiratory
803 innate immune cell function. *Am J Physiol Lung Cell Mol Physiol* **313**, L278-L292,
804 doi:10.1152/ajplung.00452.2016 (2017).
- 805 10 Clapp, P. W. et al. Cinnamaldehyde in flavored e-cigarette liquids temporarily
806 suppresses bronchial epithelial cell ciliary motility by dysregulation of mitochondrial
807 function. *Am J Physiol Lung Cell Mol Physiol* **316**, L470-L486,
808 doi:10.1152/ajplung.00304.2018 (2019).
- 809 11 Madison, M. C. et al. Electronic cigarettes disrupt lung lipid homeostasis and innate
810 immunity independent of nicotine. *J Clin Invest* **129**, 4290-4304, doi:10.1172/jci128531
811 (2019).
- 812 12 Ghosh, A. et al. Chronic E-Cigarette Use Increases Neutrophil Elastase and Matrix
813 Metalloprotease Levels in the Lung. *Am J Respir Crit Care Med*,
814 doi:10.1164/rccm.201903-0615OC (2019).
- 815 13 Sussan, T. E. et al. Exposure to electronic cigarettes impairs pulmonary anti-bacterial
816 and anti-viral defenses in a mouse model. *PLoS One* **10**, e0116861,
817 doi:10.1371/journal.pone.0116861 (2015).
- 818 14 Gerloff, J. et al. Inflammatory Response and Barrier Dysfunction by Different e-Cigarette
819 Flavoring Chemicals Identified by Gas Chromatography-Mass Spectrometry in e-Liquids
820 and e-Vapors on Human Lung Epithelial Cells and Fibroblasts. *Appl In Vitro Toxicol* **3**, 28-
821 40, doi:10.1089/aitv.2016.0030 (2017).

- 822 15 Muthumalage, T. *et al.* Inflammatory and Oxidative Responses Induced by Exposure to
823 Commonly Used e-Cigarette Flavoring Chemicals and Flavored e-Liquids without
824 Nicotine. *Front Physiol* **8**, 1130, doi:10.3389/fphys.2017.01130 (2017).
- 825 16 Behar, R. Z., Luo, W., McWhirter, K. J., Pankow, J. F. & Talbot, P. Analytical and
826 toxicological evaluation of flavor chemicals in electronic cigarette refill fluids. *Sci Rep* **8**,
827 8288, doi:10.1038/s41598-018-25575-6 (2018).
- 828 17 Clapp, P. W. *et al.* Cinnamaldehyde in Flavored E-Cigarette Liquids Temporarily
829 Suppresses Bronchial Epithelial Cell Ciliary Motility by Dysregulation of Mitochondrial
830 Function. *Am J Physiol Lung Cell Mol Physiol*, doi:10.1152/ajplung.00304.2018 (2019).
- 831 18 Hickman, E., Herrera, C. A. & Jaspers, I. Common E-Cigarette Flavoring Chemicals Impair
832 Neutrophil Phagocytosis and Oxidative Burst. *Chemical research in toxicology* **32**, 982-
833 985, doi:10.1021/acs.chemrestox.9b00171 (2019).
- 834 19 Hwang, J. H. *et al.* Electronic cigarette inhalation alters innate immunity and airway
835 cytokines while increasing the virulence of colonizing bacteria. *J Mol Med (Berl)* **94**, 667-
836 679, doi:10.1007/s00109-016-1378-3 (2016).
- 837 20 Miyashita, L. *et al.* E-cigarette vapour enhances pneumococcal adherence to airway
838 epithelial cells. *Eur Respir J* **51**, doi:10.1183/13993003.01592-2017 (2018).
- 839 21 Man, W. H., de Steenhuijsen Piters, W. A. & Bogaert, D. The microbiota of the
840 respiratory tract: gatekeeper to respiratory health. *Nat Rev Microbiol* **15**, 259-270,
841 doi:10.1038/nrmicro.2017.14 (2017).
- 842 22 Ubags, N. D. J. & Marsland, B. J. Mechanistic insight into the function of the microbiome
843 in lung diseases. *Eur Respir J* **50**, doi:10.1183/13993003.02467-2016 (2017).
- 844 23 Charlson, E. S. *et al.* Disordered microbial communities in the upper respiratory tract of
845 cigarette smokers. *PLoS One* **5**, e15216, doi:10.1371/journal.pone.0015216 (2010).
- 846 24 Ramakrishnan, V. R., Hauser, L. J. & Frank, D. N. The sinonasal bacterial microbiome in
847 health and disease. *Curr Opin Otolaryngol Head Neck Surg* **24**, 20-25,
848 doi:10.1097/moo.0000000000000221 (2016).
- 849 25 Grønseth, R. *et al.* Protected sampling is preferable in bronchoscopic studies of the
850 airway microbiome. *ERJ Open Research* **3**, 00019-02017, doi:10.1183/23120541.00019-
851 2017 (2017).
- 852 26 Di Stadio, A. *et al.* The Microbiota/Host Immune System Interaction in the Nose to
853 Protect from COVID-19. *Life (Basel)* **10**, 345, doi:10.3390/life10120345 (2020).
- 854 27 Rosas-Salazar, C. *et al.* SARS-CoV-2 Infection and Viral Load are Associated with the
855 Upper Respiratory Tract Microbiome. *J Allergy Clin Immunol*,
856 doi:10.1016/j.jaci.2021.02.001 (2021).
- 857 28 Gilbert, J. A. *et al.* Current understanding of the human microbiome. *Nature Medicine*
858 **24**, 392-400, doi:10.1038/nm.4517 (2018).
- 859 29 Li, H. in *Handbook of Statistical Genomics* 977-550 (2019).
- 860 30 Jiang, D. *et al.* Microbiome Multi-Omics Network Analysis: Statistical Considerations,
861 Limitations, and Opportunities. *Frontiers in Genetics* **10**, doi:10.3389/fgene.2019.00995
862 (2019).
- 863 31 Gloor, G. B., Macklaim, J. M., Pawlowsky-Glahn, V. & Egoscue, J. J. Microbiome Datasets
864 Are Compositional: And This Is Not Optional. *Frontiers in Microbiology* **8**,
865 doi:10.3389/fmicb.2017.02224 (2017).

- 866 32 Hinton, A. L. & Mucha, P. J. A simultaneous feature selection and compositional
867 association test for detecting sparse associations in high-dimensional metagenomic data
868 (PREPRINT - Version 1). *PREPRINT Version 1 available at Research Square*,
869 doi:<https://doi.org/10.21203/rs.3.rs-703177/v1> (2021).
- 870 33 Rebuli, M. E., Speen, A. M., Clapp, P. W. & Jaspers, I. Novel applications for a
871 noninvasive sampling method of the nasal mucosa. *Am J Physiol Lung Cell Mol Physiol*
872 **312**, L288-L296, doi:10.1152/ajplung.00476.2016 (2017).
- 873 34 Muhlebach, M. S. *et al.* Initial acquisition and succession of the cystic fibrosis lung
874 microbiome is associated with disease progression in infants and preschool children.
875 *PLoS Pathog* **14**, e1006798, doi:10.1371/journal.ppat.1006798 (2018).
- 876 35 Horvath, K. M. *et al.* Nasal lavage natural killer cell function is suppressed in smokers
877 after live attenuated influenza virus. *Respir Res* **12**, 102, doi:10.1186/1465-9921-12-102
878 (2011).
- 879 36 Davis, N. M., Proctor, D. M., Holmes, S. P., Relman, D. A. & Callahan, B. J. Simple
880 statistical identification and removal of contaminant sequences in marker-gene and
881 metagenomics data. *Microbiome* **6**, 226, doi:10.1186/s40168-018-0605-2 (2018).
- 882 37 Drengenes, C. *et al.* Laboratory contamination in airway microbiome studies. *BMC*
883 *Microbiol* **19**, 187, doi:10.1186/s12866-019-1560-1 (2019).
- 884 38 Quinn, T. P. *et al.* A field guide for the compositional analysis of any-omics data.
885 *GigaScience* **8**, doi:10.1093/gigascience/giz107 (2019).
- 886 39 Tsilimigras, M. C. B. & Fodor, A. A. Compositional data analysis of the microbiome:
887 fundamentals, tools, and challenges. *Annals of Epidemiology* **26**, 330-335,
888 doi:10.1016/j.annepidem.2016.03.002 (2016).
- 889 40 Aitchison, J. The Statistical Analysis of Compositional Data. *Journal of the Royal*
890 *Statistical Society. Series B (Methodological)* **44**, 139-177 (1982).
- 891 41 Martín-Fernandez, J. A., Barcelo-Vidal, C. & Pawlowsky-Glahn, V. Dealing with Zeros and
892 Missing Values in Compositional Data Sets Using Nonparametric Imputation.
893 *Mathematical Geology*, 26 (2003).
- 894 42 Legendre, P. & Legendre, L. in *Developments in Environmental Modelling* Vol. 24 625-
895 710 (Elsevier, 2012).
- 896 43 Oksanen, J. *et al.* Vegan: Community Ecology Package. *R Package Version 2.2-1* **2**, 1-2
897 (2015).
- 898 44 Rizzo, M. L. & Székely, G. J. Energy distance. *Wiley Interdisciplinary Reviews: Computational Statistics* **8**, 27-38, doi:10.1002/wics.1375 (2016).
- 900 45 Greenacre, M. Variable Selection in Compositional Data Analysis Using Pairwise
901 Logratios. *Mathematical Geosciences* **51**, 649-682, doi:10.1007/s11004-018-9754-x
902 (2019).
- 903 46 Ernst, M. D. Permutation Methods: A Basis for Exact Inference. *Statistical Science* **19**,
904 676-685, doi:10.1214/088342304000000396 (2004).
- 905 47 Bastian, M., Heymann, S. & Jacomy, M. *Gephi: An Open Source Software for Exploring*
906 *and Manipulating Networks*. (2009).
- 907 48 Csardi, G. & Nepusz, T. The Igraph Software Package for Complex Network Research.
908 *InterJournal Complex Systems*, 1695 (2005).

- 909 49 Anderson, M. J. in *Wiley StatsRef: Statistics Reference Online* 1-15 (American Cancer
910 Society, 2017).
- 911 50 Barker, M. & Rayens, W. Partial least squares for discrimination. *Journal of
912 Chemometrics* **17**, 166-173, doi:<https://doi.org/10.1002/cem.785> (2003).
- 913 51 Brereton, R. G. & Lloyd, G. R. Partial least squares discriminant analysis: taking the magic
914 away. *Journal of Chemometrics* **28**, 213-225, doi:<https://doi.org/10.1002/cem.2609>
915 (2014).
- 916 52 Kalivodová, A. *et al.* PLS-DA for compositional data with application to metabolomics.
917 *Journal of Chemometrics* **29**, 21-28, doi:<https://doi.org/10.1002/cem.2657> (2015).
- 918 53 Boulesteix, A.-L. & Strimmer, K. Partial least squares: a versatile tool for the analysis of
919 high-dimensional genomic data. *Briefings in Bioinformatics* **8**, 32-44,
920 doi:10.1093/bib/bbl016 (2006).
- 921 54 Kuhn, M. Building Predictive Models in R Using the **caret** Package. *Journal of Statistical
922 Software* **28**, doi:10.18637/jss.v028.i05 (2008).
- 923 55 Wickham, H. *ggplot2: Elegant Graphics for Data Analysis*. 2 edn, (Springer International
924 Publishing, 2016).
- 925 56 Fawcett, T. An introduction to ROC analysis. *Pattern Recognition Letters* **27**, 861-874,
926 doi:10.1016/j.patrec.2005.10.010 (2006).
- 927 57 Hand, D. J. & Till, R. J. A Simple Generalisation of the Area Under the ROC Curve for
928 Multiple Class Classification Problems. *Machine Learning* **45**, 171-186,
929 doi:10.1023/A:1010920819831 (2001).
- 930 58 Stone, M. Cross-Validatory Choice and Assessment of Statistical Predictions. *Journal of
931 the Royal Statistical Society: Series B (Methodological)* **36**, 111-133,
932 doi:<https://doi.org/10.1111/j.2517-6161.1974.tb00994.x> (1974).
- 933 59 Robin, X. *et al.* pROC: an open-source package for R and S+ to analyze and compare ROC
934 curves. *BMC Bioinformatics* **12**, 77, doi:10.1186/1471-2105-12-77 (2011).
- 935 60 Benjamini, Y. & Hochberg, Y. Controlling the False Discovery Rate: A Practical and
936 Powerful Approach to Multiple Testing. *Journal of the Royal Statistical Society. Series B
937 (Methodological)* **57**, 289-300 (1995).
- 938 61 Kumpitsch, C., Koskinen, K., Schöpf, V. & Moissl-Eichinger, C. The microbiome of the
939 upper respiratory tract in health and disease. *BMC Biol* **17**, 87, doi:10.1186/s12915-019-
940 0703-z (2019).
- 941 62 De Boeck, I. *et al.* Comparing the Healthy Nose and Nasopharynx Microbiota Reveals
942 Continuity As Well As Niche-Specificity. *Frontiers in microbiology* **8**, 2372-2372,
943 doi:10.3389/fmicb.2017.02372 (2017).
- 944 63 McMurdie, P. J. & Holmes, S. phyloseq: an R package for reproducible interactive
945 analysis and graphics of microbiome census data. *PLoS One* **8**, e61217,
946 doi:10.1371/journal.pone.0061217 (2013).
- 947 64 Reboli, M. E. *et al.* Wood Smoke Exposure Alters Human Inflammatory Responses to
948 Viral Infection in a Sex-Specific Manner: A Randomized, Placebo-Controlled Study. *Am J
949 Respir Crit Care Med*, doi:10.1164/rccm.201807-1287OC (2018).
- 950 65 Cho, Y. *et al.* Sex Differences in Pulmonary Responses to Ozone in Mice. Role of the
951 Microbiome. *Am J Respir Cell Mol Biol* **60**, 198-208, doi:10.1165/rcmb.2018-0099OC
952 (2019).

- 953 66 Yu, G. *et al.* The effect of cigarette smoking on the oral and nasal microbiota.
954 67 *Microbiome* **5**, 3, doi:10.1186/s40168-016-0226-6 (2017).
- 955 67 Piewngam, P. *et al.* Pathogen elimination by probiotic Bacillus via signalling interference.
956 68 *Nature* **562**, 532-537, doi:10.1038/s41586-018-0616-y (2018).
- 957 68 Liu, C. M. *et al.* *Staphylococcus aureus* and the ecology of the nasal microbiome. *Science Advances* **1**, e1400216, doi:10.1126/sciadv.1400216 (2015).
- 959 69 Sakr, A., Brégeon, F., Mège, J.-L., Rolain, J.-M. & Blin, O. *Staphylococcus aureus* Nasal
960 Colonization: An Update on Mechanisms, Epidemiology, Risk Factors, and Subsequent
961 Infections. *Frontiers in microbiology* **9**, 2419-2419, doi:10.3389/fmicb.2018.02419
962 (2018).
- 963 70 Actor, J. K., Hwang, S. A. & Kruzel, M. L. Lactoferrin as a natural immune modulator. *Curr Pharm Des* **15**, 1956-1973, doi:10.2174/138161209788453202 (2009).
- 965 71 Casimir, G. J., Lefevre, N., Corazza, F. & Duchateau, J. Sex and inflammation in
966 respiratory diseases: a clinical viewpoint. *Biology of sex differences* **4**, 16,
967 doi:10.1186/2042-6410-4-16 (2013).
- 968 72 Man, W. H. *et al.* Bacterial and viral respiratory tract microbiota and host characteristics
969 in children with lower respiratory tract infections: a matched case-control study. *Lancet Respir Med* **7**, 417-426, doi:10.1016/s2213-2600(18)30449-1 (2019).
- 971 73 Neumann, A., Björck, L. & Frick, I.-M. Finegoldia magna, an Anaerobic Gram-Positive
972 Bacterium of the Normal Human Microbiota, Induces Inflammation by Activating
973 Neutrophils. *Frontiers in Microbiology* **11**, doi:10.3389/fmicb.2020.00065 (2020).
- 974 74 Hoggard, M. *et al.* Chronic Rhinosinusitis and the Evolving Understanding of Microbial
975 Ecology in Chronic Inflammatory Mucosal Disease. *Clinical Microbiology Reviews* **30**,
976 321, doi:10.1128/CMR.00060-16 (2017).
- 977 75 Chiu, C.-Y. *et al.* Cross-talk between airway and gut microbiome links to IgE responses to
978 house dust mites in childhood airway allergies. *Scientific Reports* **10**, 13449,
979 doi:10.1038/s41598-020-70528-7 (2020).
- 980 76 Bacci, G. *et al.* Pyrosequencing Unveils Cystic Fibrosis Lung Microbiome Differences
981 Associated with a Severe Lung Function Decline. *PLoS One* **11**, e0156807,
982 doi:10.1371/journal.pone.0156807 (2016).
- 983 77 Zanger, U. M. & Schwab, M. Cytochrome P450 enzymes in drug metabolism: Regulation
984 of gene expression, enzyme activities, and impact of genetic variation. *Pharmacology &*
985 *Therapeutics* **138**, 103-141, doi:<https://doi.org/10.1016/j.pharmthera.2012.12.007>
986 (2013).
- 987 78 Vemuri, R. *et al.* The microgenderome revealed: sex differences in bidirectional
988 interactions between the microbiota, hormones, immunity and disease susceptibility.
989 *Semin Immunopathol* **41**, 265-275, doi:10.1007/s00281-018-0716-7 (2019).
- 990 79 Kim, Y. S., Unno, T., Kim, B. Y. & Park, M. S. Sex Differences in Gut Microbiota. *World J
991 Mens Health* **38**, 48-60, doi:10.5534/wjmh.190009 (2020).
- 992 80 Shin, J. H. *et al.* Serum level of sex steroid hormone is associated with diversity and
993 profiles of human gut microbiome. *Res Microbiol* **170**, 192-201,
994 doi:10.1016/j.resmic.2019.03.003 (2019).
- 995 81 Han, M. K. *et al.* Female Sex and Gender in Lung/Sleep Health and Disease. Increased
996 Understanding of Basic Biological, Pathophysiological, and Behavioral Mechanisms

- 997 Leading to Better Health for Female Patients with Lung Disease. *Am J Respir Crit Care*
998 *Med* **198**, 850-858, doi:10.1164/rccm.201801-0168WS (2018).
- 999 82 De Boeck, I. *et al.* Anterior Nares Diversity and Pathobionts Represent Sinus Microbiome
1000 in Chronic Rhinosinusitis. *mSphere* **4**, e00532-00519, doi:10.1128/mSphere.00532-19
1001 (2019).
- 1002 83 Chen, Y. W. *et al.* Fine Particulate Matter Exposure Alters Pulmonary Microbiota
1003 Composition and Aggravates Pneumococcus-Induced Lung Pathogenesis. *Front Cell Dev*
1004 *Biol* **8**, 570484, doi:10.3389/fcell.2020.570484 (2020).
- 1005 84 Mariani, J. *et al.* Short-term particulate matter exposure influences nasal microbiota in a
1006 population of healthy subjects. *Environmental research* **162**, 119-126,
1007 doi:10.1016/j.envres.2017.12.016 (2018).
- 1008

Supplementary Files

This is a list of supplementary files associated with this preprint. Click to download.

- [20210716MicrobiomePaperFinalSupplement.pdf](#)